N84 27278

SAR IMAGERY OF OCEAN-WAVE SWELL TRAVELING IN AN ARBITRARY DIRECTION

Clifford L. Rufenach
NOAA/ERL/Wave Propagation Laboratory
Boulder, Colorado 80303

Robert A. Shuchman and David R. Lyzenga
Radar Science Laboratory
Environmental Research Institue of Michigan
Ann Arbor, Michigan 48107

ABSTRACT

The intensity wave-like patterns observed in Synthetic Aperture Radar (SAR) are known to be caused by two mechanisms: the microwave radar cross-sectional amplitude modulation due to tilt and hydrodynamic interaction of the long ocean waves, and intensity modulation due to the motion of the long ocean waves. Two-dimensional closed form expressions of intensity wave patterns based on ocean wave swell are developed. They illustrate the relative importance of the amplitude and motion modulations; furthermore, they show that velocity bunching and a distortion due to the phase velocity of the ocean wave field are independent of the focus adjustment, provided that the second-order temporal effects are neglected. Second-order effects are small only over a limited range of ocean/radar parameters. Future modeling work should concentrate on two-dimensional expressions and numerical methods, including the anisotropy of the amplitude modulation, that will allow quantitatively compared with measurements.

1. INTRODUCTION

The interpretation of ocean wave imagery is an area of active research in microwave remote sensing of the ocean surface. The principles of Synthetic Aperture Radar (SAR) are well understood for point targets; see, for example, Raney (1971). However, SAR signatures caused by random and systematic motion of an extended surface such as the ocean are not as well understood but are of considerable interest.

To construct a SAR image, the radar utilizes the Doppler shift or equivalently its phase history, produced by the uniform platform velocity, to locate targets in the flight direction. If the targets move during the time interval required to form the phase history, then the history is modified and target locations differ from the ones expected for stationary targets. Suppose that an ensemble of targets are moving uniformly in the flight direction; then there is no relative position error between the targets. However, suppose that targets exist that are spatially separated in the flight direction with different radial velocity components. The radar then senses the displaced Doppler histories in the flight direction, by a process called "velocity bunching." This bunching, which is unique to the SAR, can allow the detection of ocean waves and ocean-current boundaries even when the radar cross section is uniform. However, second-order temporal (quadratic phase) effects that include the random nature of the surface also called scene coherence and the

orbital acceleration of the long waves can degrade the wave imaging process caused by velocity bunching.

The previous interpretation of ocean wave imagery has usually emphasized the image formation process along the flight direction, while others have considered the two orthogonal directions, along the flight and cross-flight slant range directions (see, e.g., Alpers and Rufenach (1979); Jain (1981); Valenzuela (1980); Harger (1980); Alpers et al. (1981). The purpose of the present work is to extend earlier results to ocean waves traveling in an arbitrary direction and include the motion of temporal amplitude modulation. To accomplish this generalization, it is necessary to develop a two-dimensional, analytical expression based on the two mechanisms responsible for wave-like patterns in the imagery: (1) the cross-sectional modulation due to tilt and hydrodynamic effects, also called amplitude modulation or the modulation transfer function, and (2) the intensity modulation due to ocean wave motions. The relative importance of amplitude and artificial modulation based on an arbitrary long ocean wave orientation must be included for quantitative modeling. Furthermore, for typical ocean/radar parameters, the image formation process is non-linear except for limited ocean-wave parameters. Therefore, a closed form expression for this mapping is not usually available except for the case when the mapping is linear. However, a two-dimensional description is useful because it gives physical insight even under the above restrictions.

Jain (1981), and Shuchman and Zelenka (1978) have made specialized measurements where the maximum image contrast occurs at a focus adjustment different than expected for a stationary surface. SAR images are brought into focus at the focal (reference) plane by adjusting the matched filter chirp rates such that $\Delta b_x = \Delta b_r = 0$ in Eq. (6). Jain (1981) has suggested that this defocus is equal to the azimuthal component of the long wave phase velocity; whereas Alpers et al. (1981) has suggested that it is the radial component of the orbital acceleration of long ocean waves that causes this defocus. The expressions developed in the present work may help resolve the focus adjustment discrepancy. Also, we show that the amplitude modulation, which is not a focusing phenomenon, can also cause distortions in the inferred ocean wave field which may be important for slow flying aircraft measurements. Furthermore, the two-dimensional encountered wave-like patterns are given in terms of the apparent ocean wavelength and direction caused by the phase velocity of ocean wave swell which is relevant for both synthetic and real aperture radars.

2. SYSTEM MODEL

Suppose that a radar platform is moving with velocity V along the x direction. Furthermore, assume that a point radar scatterer is located at a range r on the surface at x, y, and at a range R at midbeam, x = Vt, as illustrated in Fig. 1. The surface elevation associated with the wave field is

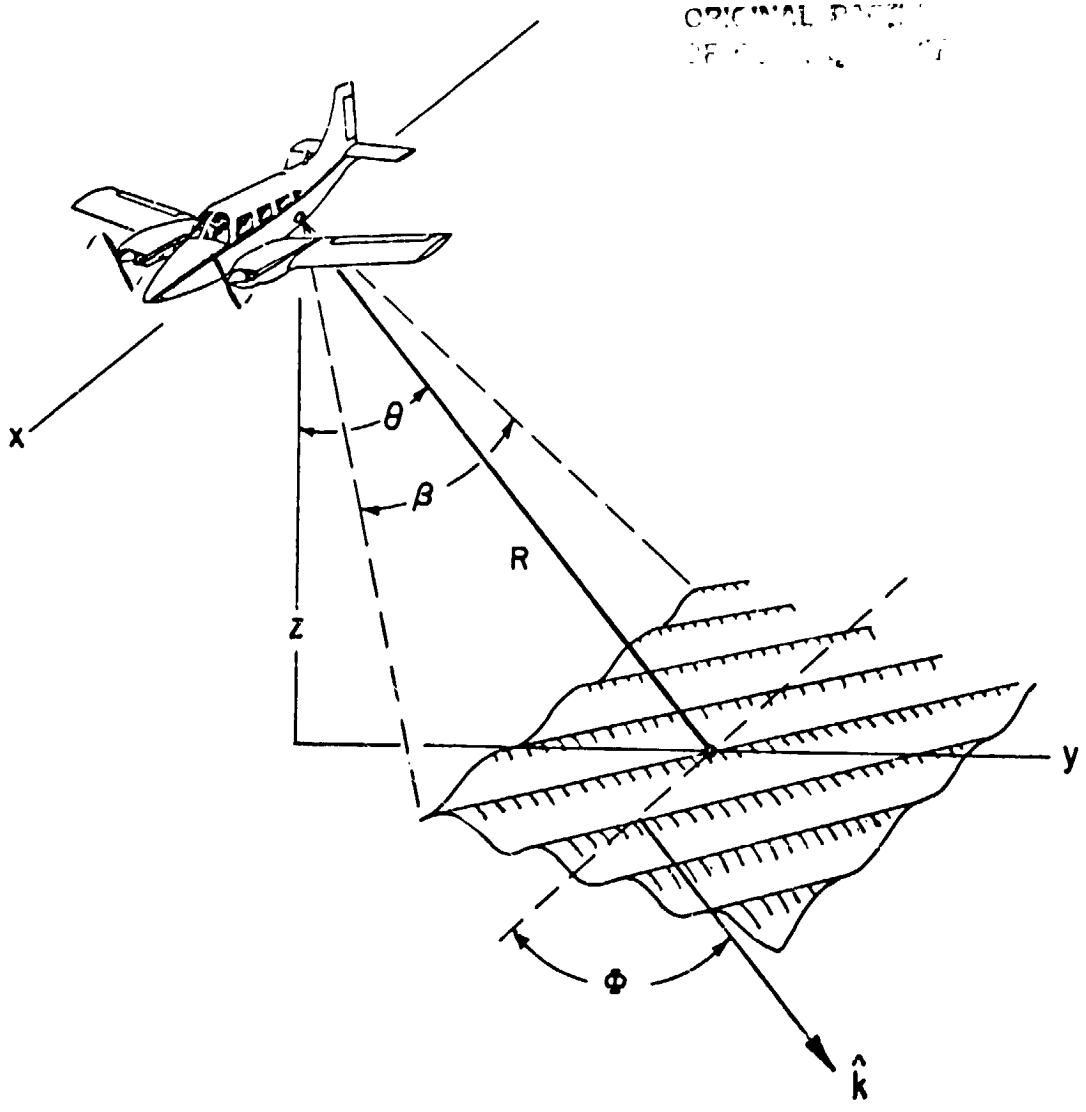

Figure 1. Artist's concept of radar/ocean geometry; θ is the angle of incidence, Φ is the azimuth angle between $\underline{k}$ the long ocean wave number and the flight direction and β is antenna beamwidth. A component of the long waves is traveling in the same direction as the flight direction; i.e., $\Phi \neq 90°$.

$$\zeta(x,y,t) = \sum_{n=1}^{\infty} r_n \cos(k_{xn}x + k_{yn}y \quad \omega_n t) \tag{1}$$

where the ocean wavenumbers k_{xn}, k_{yn} are the components along the x- and y-directions, respectively, $k_{xn} = k_n \cos \Phi_n$, $k_y = k_n \sin \Phi_n$, and $k_n = \sqrt{k_{xn}^2 + k_{yn}^2}$.

The complex amplitude signal backscattered from the ocean surface depends on the reflectivity properties of the surface including the time dependence of

the amplitude modulation due to the long ocean waves. The complex amplitude received at the platform based on a point scatterer, following Hasselmann (1980), is

$$dA(t,\tau) = G(x - Vt, y)\, E(\tau - \tau')\, e^{-i(b_y t^2 + b_r \tau^2)}\, a(x,y,t,\, dxdy \qquad (2)$$

where G is a factor that includes the antenna-weighting function $E(\tau)$ is the pulse-weighting function, b_x is the azimuth chirp rate, b_r is the range chirp rate, and $a(x,y,t)$ is the complex amplitude reflectivity. The dependence of $A(t,\tau)$ on τ (fast time) is used in processing to determine the slant range-r positions of the scattering element; the Doppler signature is related to the platform velocity and slow variability of the reflective surface through t (slow time) to infer the aximuthal x-position of the scattering element.

The received signal is compared with a reference signal in the processor which is also called a matched filter represented here by $h(t,\tau)$. The two-dimensional convolution whose output is the image complex amplitude for a point scatterer is

$$\Delta(t-t',\ \tau-\tau') = \iint A(t_1 - t\ \tau_1 - \tau\ )\, h(t'-t_1,\ \tau'-\tau_1)\, dt_1 d\tau_1 \ . \qquad (3)$$

Backscattered microwave signals from the rough sea surface are described by a two-scale Bragg scattering model first introduced by Wright (1968) and Bass et al. (1968). This model is consistent with wavelike amplitude patterns observed in imaging radar, provided that the radar resolution is smaller than the long ocean wavelength. Initially, this amplitude modulation was explained by the geometric tilting of the long ocean waves in a local reference plane. Some years later, after more complete analysis, it was shown that the straining of the short (say 1-100 cm) waves by the long waves also influenced the modulation. This straining, also called hydrodynamic interaction, causes an asymmetrical distribution of the short waves with respect to the long waves (Keller and Wright, 1975).

An extension of the previous SAR results, which shows that the amplitude modulation is dependent on the match filtering, is more easily accomplished by restricting the model to ocean wave swell, which to a first approximation can be represented by a sinusoidal long ocean wave. This simplifies Eq. (1) to one Fourier component, $\zeta(x,y,t) = \zeta_o \cos(\hat{k}_x x + \hat{k}_y y - \hat{\omega}t)$. Therefore the complex amplitude reflectivity can be approximated by

$$a(x,y,t) \approx \left[1 + \frac{\hat{m}}{2} \cos\left(\hat{k}_x x + \hat{k}_y y - \hat{\omega}t\right)\right] e^{-i\hat{\phi}(x,y,t)} \qquad (4)$$

where $\hat{m}$ is the complex amplitude modulation index caused by the long ocean waves, $\hat{\phi}$ is the phase perturbations caused by the orbital motion, and the hat "^" indicates long ocean wave parameter. For the present model the scene coherence is neglected. The reader interested in this coherance is referred to Raney (1980), Rufenach and Alpers (1981), and Lyzenga and Shuchman (1983). The phase perturbation can usually be approximated by

$$\hat{\phi} \equiv 2k_o(\hat{u}_r t + \hat{a}_r/2\, t^2) \ , \tag{5}$$

where k_o is the radar wavenumber, and $\hat{u}_r$ and $\hat{a}_r$ are radial components of the orbital velocity and acceleration of the long waves, respectively. The amplitude modulation index can be approximated by $\dot{m} = \dot{m}_o \zeta_o \sqrt{\hat{k}_x^2 + \hat{k}_y^2}$ based on ocean wave swell where $\dot{m}_o$ is the modulation transfer function given by others (see, e.g., Keller and Wright, 1975); and dependent on ocean/radar parameters. For example, suppose the long ocean waves are traveling along the radar look direction (range traveling waves) and the receiving and transmitting antennas are horizontally polarized then $m_o \approx 4(\tan\theta + \cot\theta)$ or vertically polarized $m_o \approx -2 \sin 2\theta/(1 + \sin^2\theta) + 4 \cot\theta$ (Rufenach et al., 1983).

The image is brought into focus in a reference plane by adjusting the quadratic phase of the matched filter. In practice, this focus adjustment is usually achieved on an optical processor by adjustments of the focal length between the platform and a stationary reference surface. Therefore the matched filter is given by

$$h(t,\tau) = e^{-i(b_x' t^2 + b_r' \tau^2)} \ , \tag{6}$$

where the reference chirp rates b_x' and b_r' may differ from the received chirp rates $b_x = k_o V^2/R$ and $b_r = 2B_r/T_r$ by the differential rate $\Delta b_x = b_x' - b_x$ and $\Delta b_r = b_r' - b_r$. The received envelope of the chirp signal is related to the azimuthal bandwidth $B_x = b_x T_x/2$ and range bandwidth $B_r = b_r T_r/2$ where T_x and T_r are the azimuth integration time and the rf pulse duration, respectively.

The intensity modulation based on a point scatterer riding an ocean swell and assuming a Gaussian antenna weighting

$$G(t,\tau) = \exp\left[-\frac{2}{T_x^2}(t'-t)^2 - \frac{2}{T_r^2}(\tau'-\tau)^2\right] \tag{7}$$

is obtained by substituting Eqs. (2), (4), and (6) into Eq. (3) based on the high radar wavenumber limit ($k_o \to \infty$), and assuming $m \ll 1$. Following Rufenach and Alpers (1981), and Hasselmann (1980) for temporal-to-spatial coordinate transformation and using straightforward but tedious mathematics,

$$|\Delta|^2 = \frac{\pi}{2}\left(1 + \frac{\Delta b_x}{b_x}\right)\left(1 + \frac{\Delta b_r}{b_r}\right) T_x^2 T_r^2 \left[1 + \dot{m} \cos\left(\hat{k}_x' x + \hat{k}_r r\right)\right]$$

$$\exp\left[-\left(\frac{\pi}{\rho_x}\right)^2 \left(1 + \frac{\Delta b_x}{b_x}\right)^2 \left(x' - x + \frac{R}{V}\hat{u}_r'\right)^2 - \left(\frac{\pi}{\rho_r}\right)^2 \left(1 + \frac{\Delta b_r}{b_r}\right)(r' - r)^2\right] \quad (8)$$

where $\hat{k}_x' = \hat{k}_x\left(1 - \frac{\hat{\omega}/\hat{k}_x}{V}\right)$ is the apparent long ocean wavenumber,

c is the velocity of light

and $\rho_x = \frac{\pi}{2}\frac{V}{B_x}$,

$\rho_r = \pi \frac{c}{B_r}$,

and $\hat{u}_r' = \dfrac{\hat{u}_r}{1 + \dfrac{\Delta b_x}{b_x}}$.

The high wavenumber limit is taken with the azimuth antenna diameter constant which means that the integration time is sufficiently small that all quadratic phase effects such as orbital acceleration can be neglected. The above expressions apply for an image whose azimuth scale is equal to the radar antenna beamwidth. Equation (8) illustrates that the amplitude modulation field as measured in radar images can be distorted from the actual wave field on the ocean surface. This distortion occurs only along the flight direction. Furthermore, this distortion is not caused by a quadratic phase effect. Indeed, the type of distortion in Eq. (8) is most important for slow flying aircraft when the long ocean waves are traveling along the flight direction, relevant for both synthetic aperture and real aperture radars. Equation (8) shows the dependence of amplitude modulation on image formation based on a point scatterer riding on a monochromatic ocean wave swell.

The image response based on a distributed surface such as the ocean is obtained by summing all the elementary point scatterer contributions:

$$I(x',r') = \iint |\Delta|^2 \, dx dr \, . \quad (9)$$

Using the assumptions of Alpers and Rufenach (1979) namely

C-3

$$\dot{m},\ \hat{u}_r \text{ and } \left|1 + \frac{R}{V}\frac{d\hat{u}_r}{dx}\right| ,$$

not varying much within a resolution cell we obtain

$$I(x',r') = \frac{\pi/4\ T_x^2 T_r^2}{\left|1 + \frac{R}{V}\frac{d\hat{u}_r}{dx}\right|}\left(1 + \frac{\Delta b_x}{b_x}\right)\left(1 + \frac{\Delta b_r}{b_r}\right)\left[1 + \dot{m}_{sar}\cos\left(\hat{k}_x x' + \hat{k}_r r'\right)\right] \quad (10)$$

where $\dot{m}_{sar} = \dot{m}\exp\left[-\frac{1}{4\pi^2}\left(\hat{k}_x'^2\frac{\rho_x^2}{\left(1 + \frac{\Delta b_x}{b_x}\right)^2} + \hat{k}_r^2\frac{\rho_r^2}{\left(1 + \frac{\Delta b_r}{b_r}\right)^2}\right)\right]$.

Furthermore, if $\frac{R}{V}\frac{d\hat{u}_r}{d_x} \ll 1$ then Eq. (10) simplifies to

$$I(x',r') \approx K\left(1 - \frac{R}{V}\frac{d\hat{u}_r}{d_x}\right)\left[1 + \dot{m}_{sar}\cos\left(\hat{k}_x x' + \hat{k}_r r'\right)\right] \quad (11)$$

where $K = \pi/4\ T_x^2\ T_r^2\left(1 + \frac{\Delta b_x}{b_x}\right)\left(1 + \frac{\Delta b_r}{b_r}\right)$ or in terms of ocean wave swell parameters

$$I(x',r') \approx K\left[1 + \eta_o\cos\left(k_x x' + k_r r'\right) + \left|\dot{m}_{sar}\right|\cos\left(k_x x' + k_r r' + \delta\right)\right] \quad (12)$$

where $\eta_o = R/V\ \zeta_o\ \hat{\omega}\ \hat{k}_x\sqrt{\sin^2\theta\ \sin^2\phi + \cos^2\theta}$ is the amplitude of the velocity bunching, $\left|\dot{m}_{sar}\right| \cong m_o r_o\sqrt{\hat{k}_x^2 + \hat{k}_y^2}$ provided the radar resolution filtering of the long waves is neglected, and δ is the phase angle of the amplitude modulation. For tilt modulation $\delta = \pi/2$, which means that the surface elevation is 90° out of phase with the amplitude modulation. Equations (10) and (11) show that wave-like patterns in the image caused by ocean wave swell are due to two mechanisms: velocity bunching and amplitude modulation. These equations hold only over a narrow range of ocean/radar parameters since quadratic effects such as orbital acceleration have been neglected. However, they do illustrate the relative importance of the real and artificial modulations. The amplitude modulation is the factor within the square brackets in Eqs. (10) and (11). Equation (11) and (12) are linear expressions relating the wave field to the image intensity modulation.

The Synthetic Aperture Radar is generally considered to be a sensor that can measure the dominant ocean wavelength and direction. Under certain limited conditions, significant distortions can occur in both the observed wavelength and direction. Using Eq. (10) or (11) gives

$$\hat{k}_x' = \hat{k}_x - \hat{\omega}/V \tag{12}$$

$$\hat{k}_y' = \hat{k}_y \tag{13}$$

where primed parameters indicate apparent parameters, whereas the unprimed parameters refer to the actual wavefield. Therefore, the apparent wavelength is

$$\hat{\lambda}' = \hat{\lambda} \left| 1 - \frac{\hat{\omega}/\hat{k}_x}{V} \right| \tag{14}$$

where $\hat{\lambda}' = 2\pi/\hat{k}'$ and $\hat{k} = \dfrac{\hat{k}_x}{\cos\hat{\Phi}}$,

and the apparent direction is

$$\hat{\Phi}' = \tan^{-1} \left[\frac{\sin\hat{\Phi}}{\cos\hat{\Phi} + \dfrac{\hat{\omega}/\hat{k}}{V}} \right] . \tag{15}$$

As an example consider two cases in which deep water swell with $\hat{\lambda} = 250$ m is traveling along and opposite to the sensor flight direction. Suppose further that the sensor is a slow-flying aircraft with V = 100 m/s. The phase velocity is $\hat{\omega}/\hat{k}_x = 20$ m/s which gives $\hat{\lambda}' \cong 250\ (1 \pm 0.2) = 200, 300$ m. This illustrates that significant distortion can be due to other than non-linear effects under certain conditions. However, it should be noted that non-linearities, caused by orbital acceleration are likely to dominate on most occasions.

3. DISCUSSION AND SUMMARY

The wave-like patterns observed in SAR imagery are caused by two mechanisms: (1) the radar cross-sectional (amplitude) modulation due to tilt and hydrodynamic modulation by the long ocean waves and (2) intensity modulation due to the motion of the ocean surface which is unique to SAR. The motion-induced modulation can be separated into modulation enhancement and degradation due to the systematic orbital acceleration of the long waves and the degradation of the modulation due to the stochastic character of the wind waves. The radar amplitude modulation is dominant for ocean waves traveling perpendicular to the flight direction whereas the motion-induced modulation may dominate when ocean waves are traveling along the flight direction.

Determination of the relative importance of these underlying mechanisms is essential to a complete understanding of the radar interaction with the ocean waves and the modeling of SAR wavelike patterns; for example, see, Lyzenga et al., 1984. Interest in the different mechanisms has increased in recent years since it is difficult to separate them except for the special case when the waves are traveling exactly perpendicular to the flight direction (range

waves). For this case, motions on the surface are negligible. Most of the theoretical work has emphasized the modulation due to ocean wave motion and its associated non-linearities. A two-dimensional closed form expression is not available except over a limited range of ocean/radar parameters. This has led some workers to consider Monte Carlo numerical methods to model the image-formation process (Alpers, 1983). Two-dimensional expressions have been developed which are valid over a limited range of ocean/radar parameters. Indeed in this limited range, the Monte Carlo results that required numerical computation could be compared with closed form results such as Eqs. (10) and (11).

Equations (10) and (11) include the effects of both radar amplitude and velocity bunching modulation. These equations show the following salient features: (1) Velocity bunching is independent of focus adjustment, provided that the quadratic phase is negligibly small which normally means short integration times; however, focus adjustment will degrade the image in the same manner as in a stationary scene, and (2) Ocean wave field distortion caused by the motion of the wave field (phase velocity of the long waves) relative to the platform velocity is independent of focus adjustment, again provided that the quadratic phase is negligibly small. These conclusions are in disagreement with Jain (1981), who claims that the focus adjustment is equal to the azimuth component of the long wave phase velocity. Furthermore, the dependence of the focus adjustment on orbital acceleration as suggested by Alpers et al. (1981), is not relevant since these expressions are not valid when the orbital acceleration is important.

It is recommended that future work continue to emphasize development of quantitative two-dimensional models which give the relative importance of amplitude and motion modulation for any arbitrary orientation of the ocean wave field. Furthermore, the anisotropy of the amplitude modulation must be included in order to quantify this modulation.

ACKNOWLEDGMENTS

The NOAA portion of this work was partially supported by NASA Headquarters (Ocean Processes Branch) under work order number W-15,084. The ERIM portion of this work was supported by NASA Headquarters (Ocean Processes Branch) and ONR under contract No. N00014-81-C0692. The NASA technical monitors are Dr. Lawrence, F. McGoldrick and Dr. William Patzert and the ONR technical monitor is Mr. Hans Dolezalek.

REFERENCES

Alpers, W. R., 1983: Monte Carlo simulations for studying the relationship between ocean wave and synthetic aperture radar image spectra. J. Geophys. Res., 88(C3), 1745-1759.

Alpers, W. R., and C. L. Rufenach, 1979: The effect of orbital motions on synthetic aperture radar imagery of ocean waves. IEEE Trans. Antennas Propagat. AP-27, 685-690, September.

Alpers, W. R., R. B. Ross, and C. L. Rufenach, 1981: On the detectability of ocean surface waves by real and synthetic aperture radar. J. Geophys.

Res., 86(C7), 6481-6498.

Bass, F. G., I. M. Fuks, A. I. Kalmykov, I. E. Ostrovsky and A. D. Rosenberg, 1968: Very high frequency radiowave scattering by a disturbed sea surface. IEEE Trans. Antennas and Propagat., AP-16, 554-568.

Harger, R. O., 1980: The side-looking image of time variant scenes. Radio Sci. 15(4), 749-756.

Hasselmann, K., 1980: A simple algorithm for the direct extraction of the two-dimensional surface image spectrum from the return signal of a synthetic aperture radar. Int. J. Remote Sensing, 1(3), 219-240.

Jain, A., 1981: SAR imaging of ocean waves: Theory. IEEE J. Oceanic Eng. OE-6(4), 130-139.

Keller, W. C., and J. W. Wright, 1975: Microwave scattering and straining of wind generated waves. Radio Sci., 10, 139-147.

Lyzenga, D. R., and R. A. Shuchman, 1983: Analysis of scatter motion effects in Marsen X band SAR imagery. J. Geophys. Res. 88(C14), 9769-9775.

Lyzenga, D. R., R. A. Shuchman, J. D. Lyden and C. L. Rufenach, 1984: SAR imaging of waves in water and ice: Evidence for velocity bunching. J. Geophys. Res. accepted for publication.

Raney, R. K., 1971: Synthetic aperture imaging radar and moving targets. IEEE Trans. Aerosp. Electron. Syst., AES-7, 499-505.

Raney, R. K., 1980: SAR processing of partially coherent phenomena. IEEE Trans. Antennas Propagat. AP-28, 777-787.

Rufenach, C. L., and W. R. Alpers, 1981: Imaging ocean waves by synthetic aperture radars with long integration times. IEEE Trans. Antennas Propagat. AP-29(3), 422-428.

Rufenach, C. L., J. R. Apel, L. S. Fedor and F. I. Gonzalez, 1983: Surface and internal ocean wave observations. Advances in Geophysics, ed. Barry Saltzman, in press.

Shuchman, R. A., and J. S. Zelenka, 1978: Boundary Layer Meteorol., 13, 181-192.

Valenzuela, G. R., 1980: An asymptotic formulation for SAR images of the dynamical ocean surface. Radio Sci., 15, 105-114.

Wright, J. W., 1968: A new model for sea clutter. IEEE Trans. Antennas and Propagat., 16, 217-223.